Supplementary Data

Table 1. Demographics and patient characteristics	
Median age, years (range)	58 (33-72 years)
Race (n, %)	
White	6, 55%
Black	5, 45%
Stage at diagnosis (n, %)	
0-III	10, 91%
IV	1, 9%
Prior (neo)adjuvant therapy (n, %)	
Yes	11, 100%
No	0, 0%
Prior surgery (n, %)	
Mastectomy	9, 82%
Lumpectomy	1, 9%
Prior radiation to breast/chest wall (n, %)	
Yes	9, 82%
No	2, 18%
Prior metastatic lines of systemic therapy (n, %)	
0-3	7, 64%
4 or more	4, 46%
ECOG performance status (n, %)	
0	9, 82%
1	2, 18%

Table 2. Patient response/survival

Pt. no.	Best objective response	PFS (months)
1	CR	36.49
2	PR	7.50
3	PR	6.28
4	PR	16.31
5	PR	29.23
6	PD	2.07
7	PD	1.68
8	PD	2.53
9	PD	1.94
10	PD	2.56
11	PD	2.76

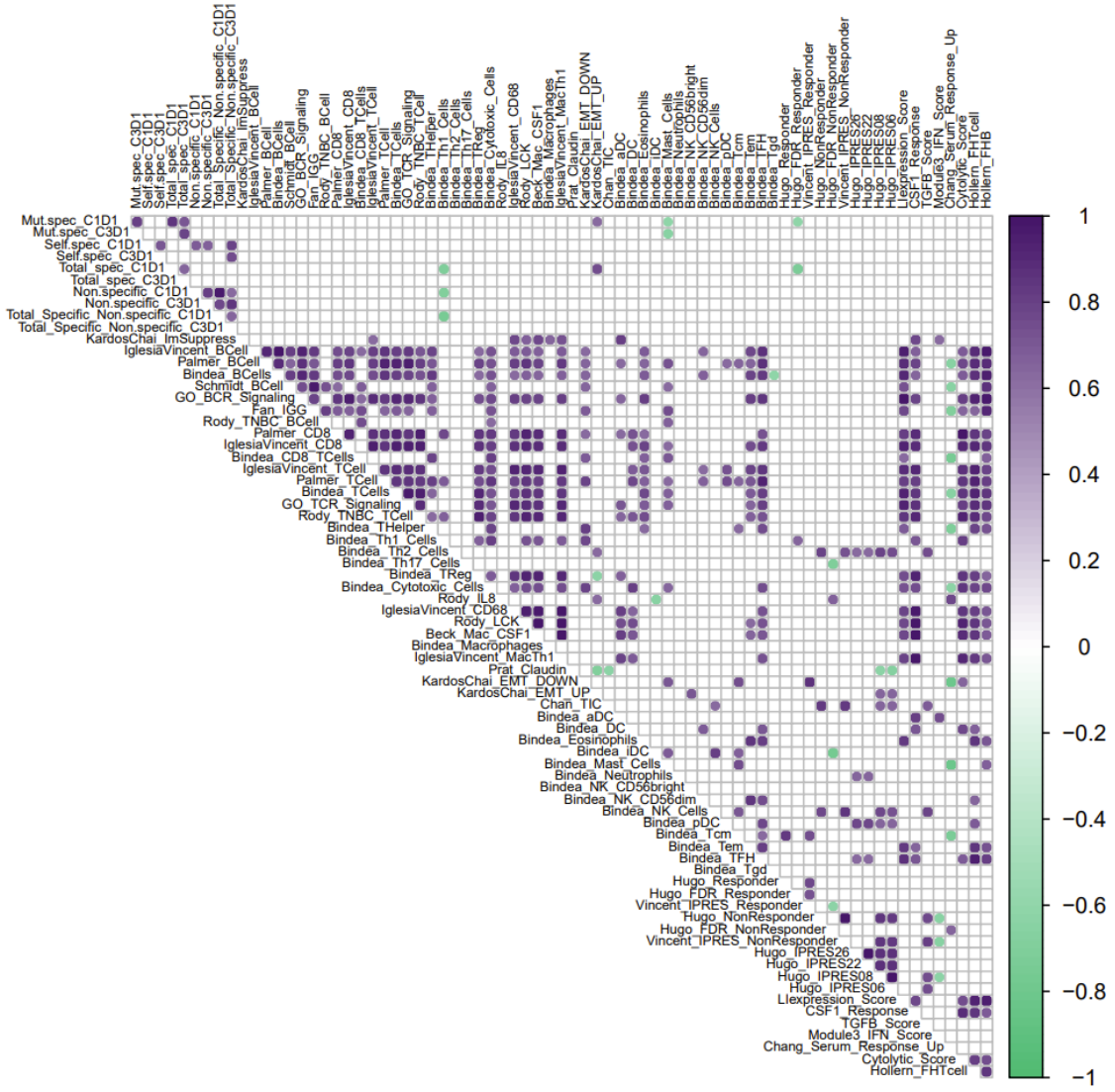

Supplementary Figure 1. Correlations of cumulative antibody response with pretreatment tumor immune gene signatures (IGS). Colored dots represent significant associations (Spearman rho, p<0.05; n=11) between antibody responses and tumor IGS (IGS described in Anders et al, doi: 10.1136/jitc-2021-003427). Values are not hierarchically clustered, such that antibody response variables are grouped together for ease of interpretation.

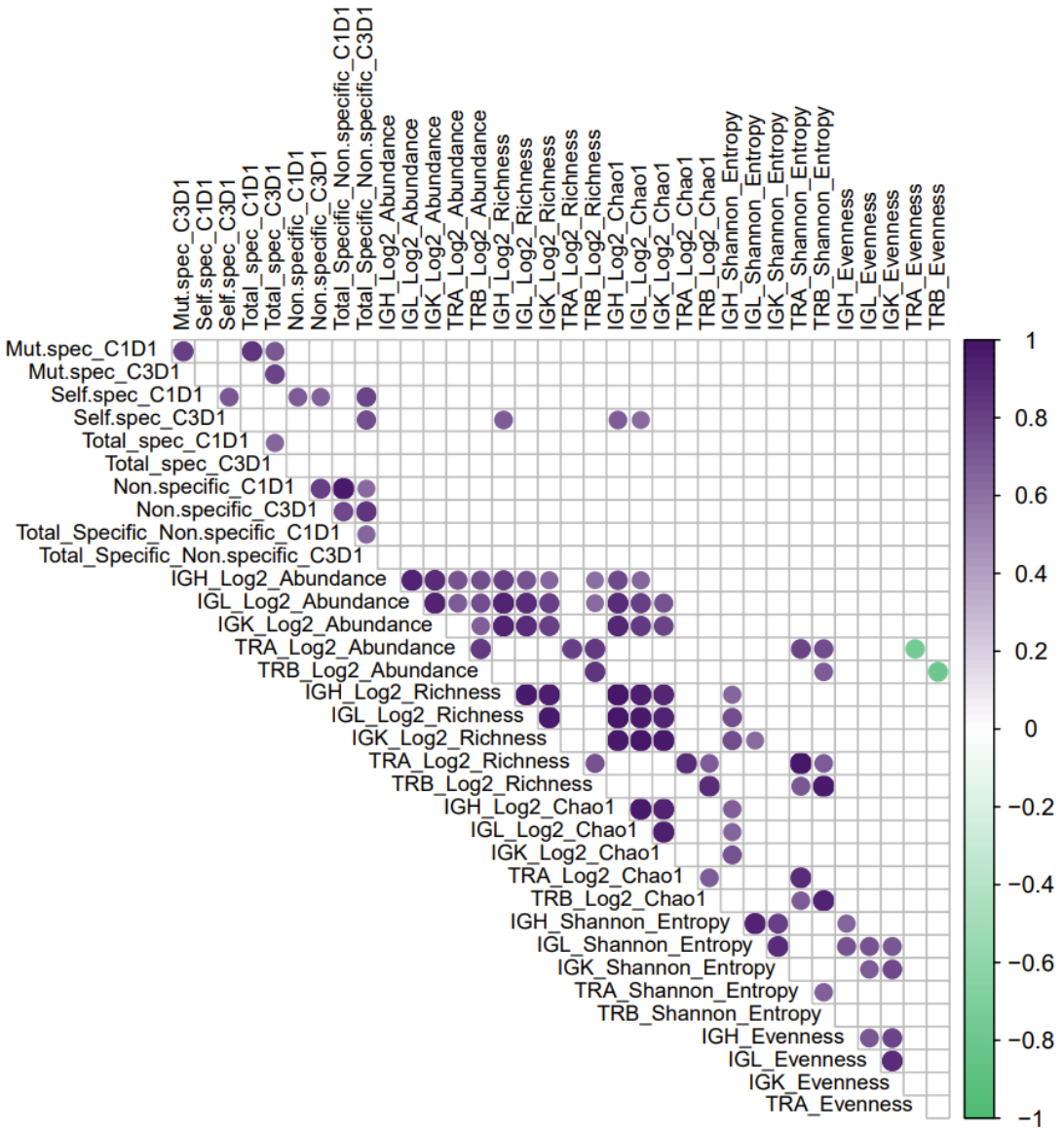

Supplementary Figure 2. Correlations of cumulative antibody response with pretreatment tumor immunogenomics features. Antibody responses correlated to pretreatment TRA, TRB, IGH, IGL, and IGK abundance/diversity metrics. Colored dots represent significant associations (Spearman rho, $p<0.05$; n=11). Values are not hierarchically clustered, such that antibody response variables are grouped together for ease of interpretation. Adaptive immune receptor repertoire analytical methods are described in detail in Anders et al (doi: 10.1136/jitc-2021-003427).

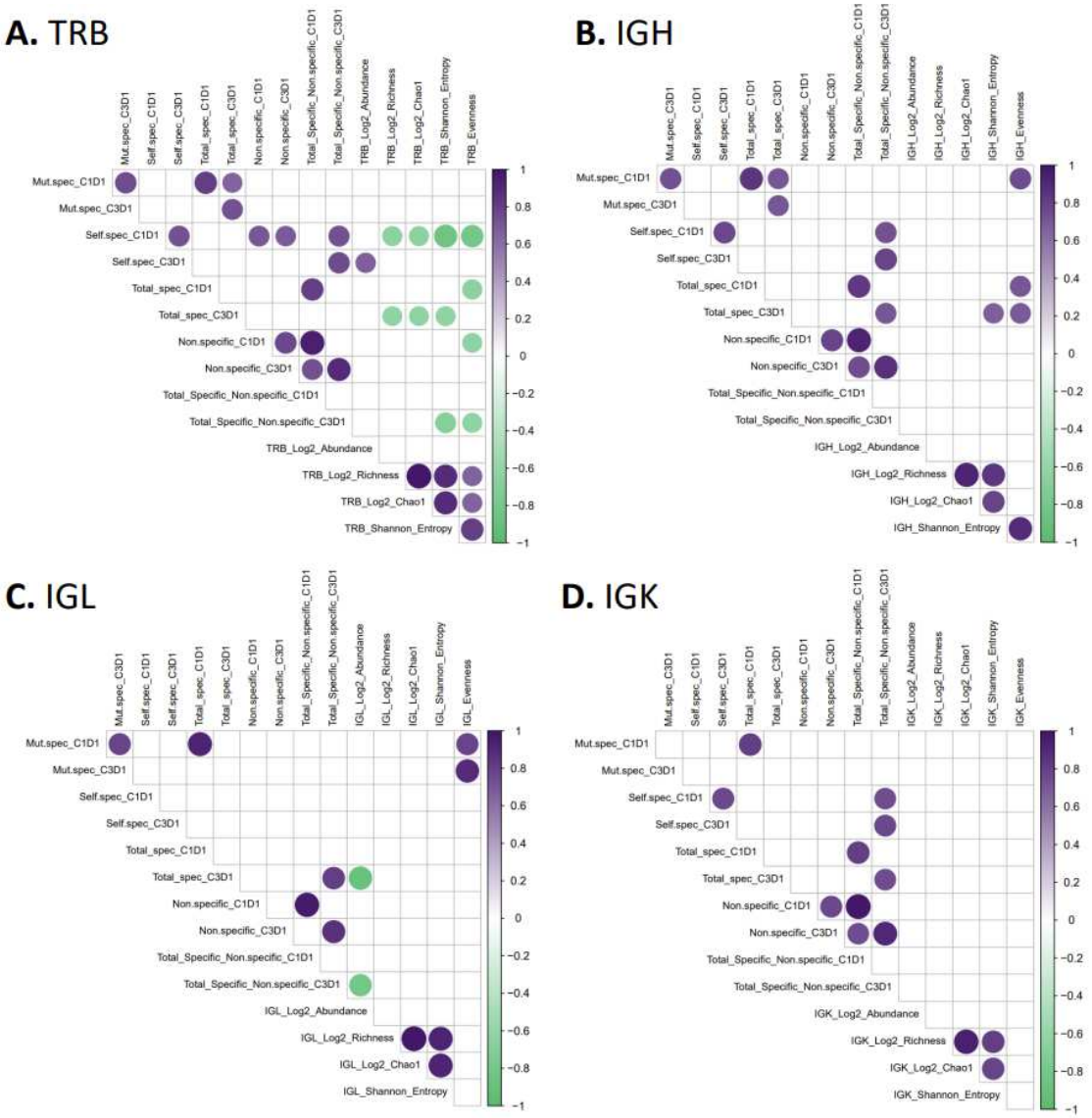

Supplementary Figure 3. Correlations of cumulative antibody response with pretreatment peripheral blood immunogenomics features. Antibody responses correlated to **(A)** TRB (n=10), **(B)** IGH (n=9), **(C)** IGL (n=7), and **(D)** IGK (n=8) abundance/diversity metrics measured from pretreatment peripheral blood; note: different *n* due to absence of detectable features in some patients. Colored dots represent significant associations (Spearman rho; p<0.05).

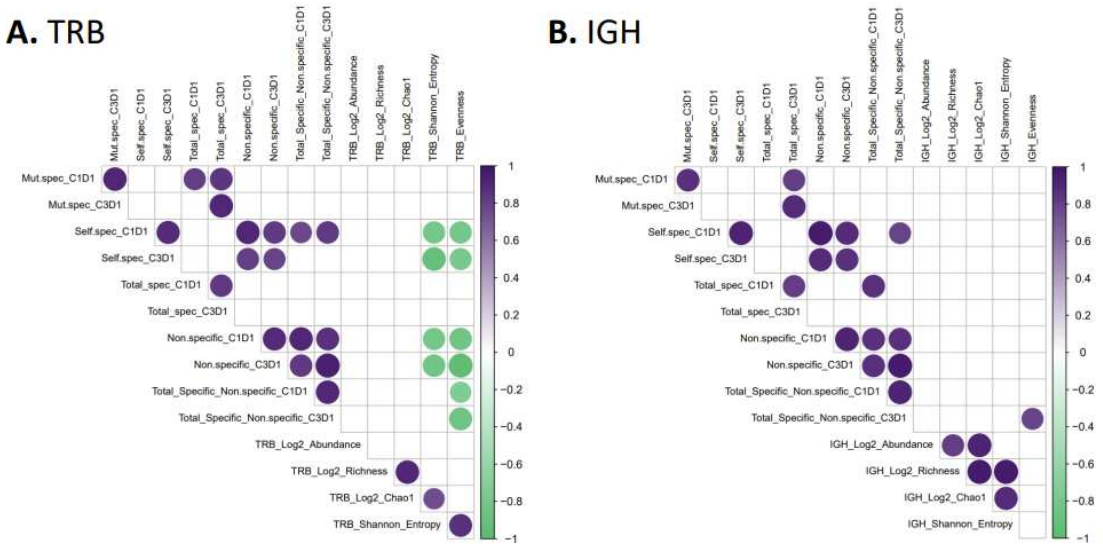

Supplementary Figure 4. Correlations of cumulative antibody response with posttreatment peripheral blood immunogenomics features. Antibody responses correlated to **(A)** TRB (n=8) and **(B)** IGH (n=7) abundance/diversity metrics measured from posttreatment peripheral blood. Note different *n* due to absence of detectable features in some patients; also, IGL/IGK not included due to lack of correlations with antibody response, likely due to low number of samples with detectable features (e.g., samples with detectable posttreatment IGL, n=4; samples with detectable posttreatment IGK, n=5). Colored dots represent significant associations (Spearman rho; p<0.05).

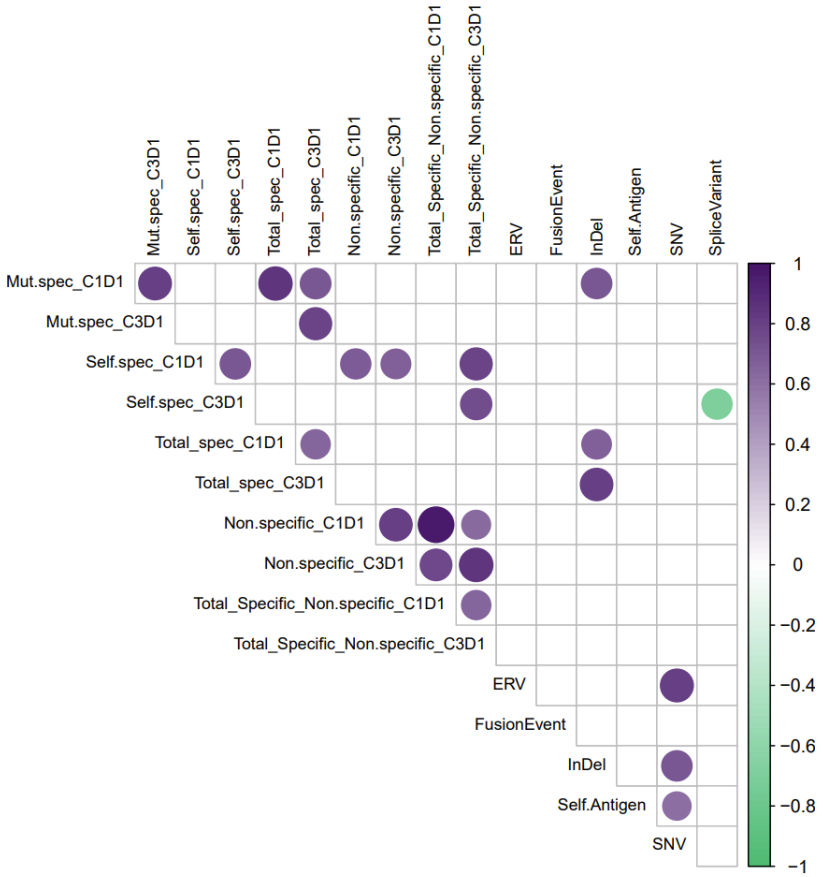

Supplementary Figure 5. Correlations of antibody response with neoantigen load, including alternative antigen sources. Correlation table of antibody response metrics relative to predicted levels of MHC Class I-restricted antigens from SNV, InDel, ERV, CTA/self-antigens, fusions, and splice variants**.** Predicted antigens were filtered based on thresholds of predicted binding affinity (<500 nM) and RNAseq reads supporting the predicted antigen peptide coding region (>0); no viral antigens were detected that passed this filtering threshold. Methods for neoantigen prediction are described in detail here: bioRxiv 2022.04.01.486738; doi: 10.1101/2022.04.01.486738).

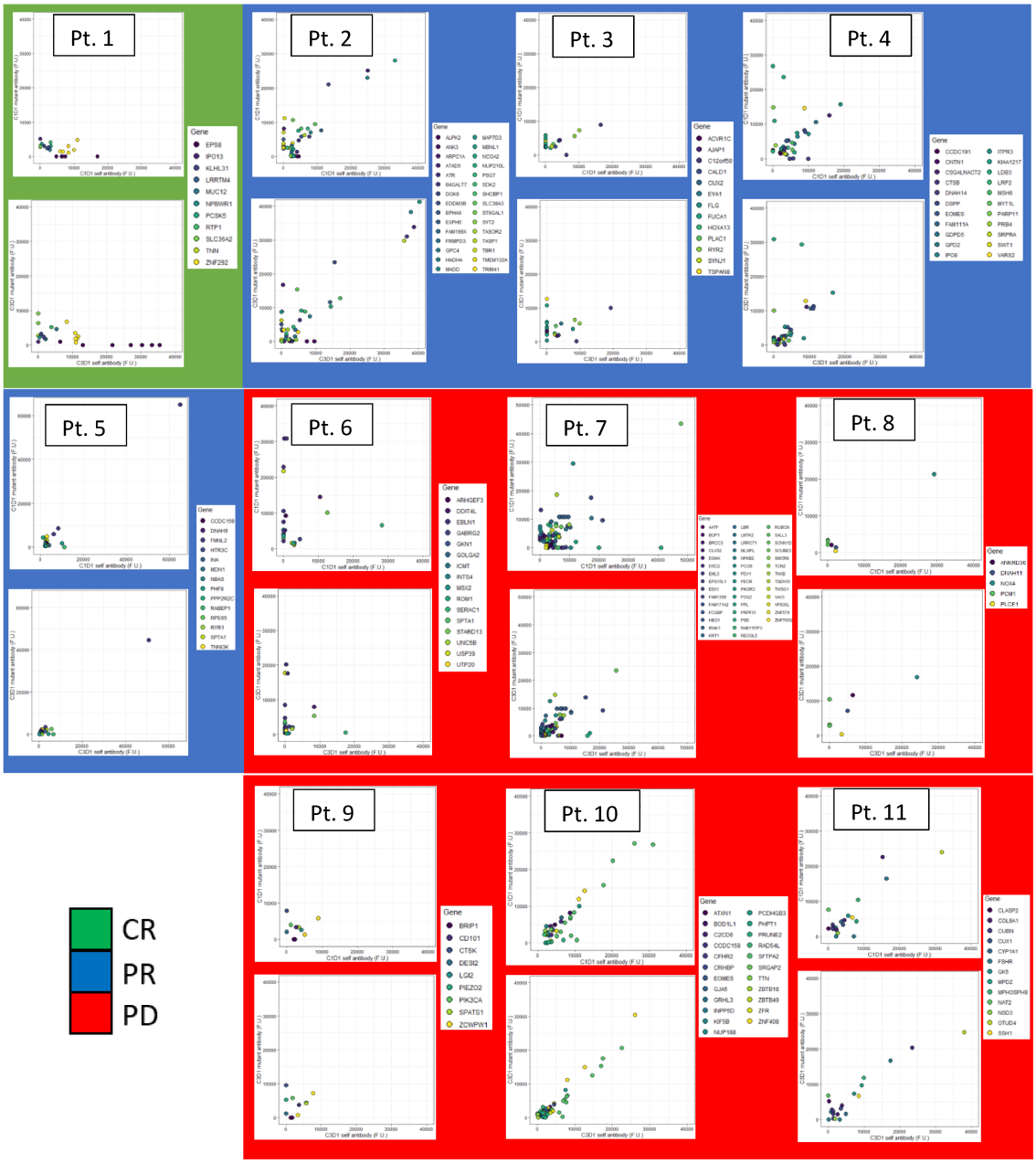

Supplementary Figure 6. Relative antibody signal to self/mutant peptide pairs at C1D1 (top) and C3D1 (bottom). For C1D1 plots, peptide pairs were excluded if signal to self-peptide was <2,000 F.U. *and* signal to mutant peptide was <2,000 F.U.; for C3D1 plots, the same peptide pairs as shown in the C1D1 plots are displayed. Colored annotation depicts parental gene product/proteins.

Supplementary Methods

Patient selection

From the patients enrolled in the LCCC1525 clinical trial (n=40), 6 responders (1 CR and 5 PR; out of a total 8 responders) and 6 non-responders (6 PD; out of a total 32 non-responders) were selected for antibody presence/response evaluation in this study. In addition to the one CR, the 5 PR were chosen randomly from the remaining 7 patients with PR. For the non-response group, we selected patients with progressive disease, as this was the large majority of non-responders in the cohort (e.g., n=28 of 32 non-responders). Of the 28 patients with PD, 20 did not have available plasma at C3D1 and were thus excluded; we thus randomly chose 6 of the remaining 8 PD patients for evaluation. One patient with PR was not included in the data analysis due to high level of non-specific background staining on the peptide array. It should be noted that the selection of only 12 patients for evaluation was driven by funding constraints.

Whole-exome sequencing and variant calling

WES was performed on FFPE tumor tissue collected prior to treatment on the LCCC1525 trial of low-dose cyclophosphamide plus pembrolizumab in metastatic triple negative breast cancer (NCT02768701), with PBMCs collected serving as the matched normal. Library preparation was performed with the TruSeq DNA, PCR-Free kit (Illumina, San Diego, California, USA) and pooled samples sequenced on the HiSeq4000 platform (Illumina). Somatic and germline WES sequencing files were aligned to Hg38 using bwa (v0.7.17) and sorted, indexed, and duplicates marked using biobambam2 (v2.0.87). BAMs were realigned with Abra2 (V.2.22), followed by somatic and germline variant detection with Strelka2 (V.2.9.10), Cadabra (from Abra2 V.2.22) and Mutect2 (GATK V.4.1.4.0). Capture of exonic sequences was verified using the Picard (V.2.21.1) CollectHsMetrics tool, and quality of sequencing data verified using FastQC (V.0.11.8), and the Picard suite's CollectAlignmentSummaryMetrics, CollectInsertSizeMetrics, QualityScoreDistribution, and MeanQualityByCycle tools. Variants were filtered by the following criteria: protein-coding mutations only, Cadabra indel quality >10.5, Mutect2 indel quality >6.8 or single nucleotide variant (SNV) quality >9.2, Strelka2 indel quality >15.2 or SNV quality >19.7. Remaining variants required at least five supporting reads and a minimum read depth of 40, or 10 supporting reads and minimum read depth of 80 if MAF <5%. Variants with a MAF >5% in normal tissue were dropped, as were variants appearing at rates above 1% in any subpopulation in either GnomAD or 1000 Genomes databases. To counter FFPE artifacts, C>T and G>A substitutions required a minimum MAF of 10%. Tumor mutational burden (TMB) was calculated from small indels and substitutions identified by WES, and divided by the megabases adequately covered by sequencing reads.

RNA sequencing

Samples of total RNA extracted from FFPE tumor tissue (ROCHE High Pure FFPE kit, Indianapolis, Indiana, USA) were used to prepare Illumina TruSeq RNA Access (Cat. No. 20020189) sequencing libraries. Sequencing was performed in the UNC- Chapel Hill High Throughput Sequencing Facility on an Illumina HiSeq 4000 platform using the Illumina HiSeq SBS 150 Cycles (PE- 410- 1001) with 2x75 paired end base reads.